Weakly Supervised Semantic Segmentation by Knowledge Graph Inference

Jia Zhang[a], Bo Peng[a,*], Xi Wu[b]

[a]*School of Computing and Artificial Intelligence, Southwest Jiaotong University, 610031 Chengdu, Sichuan, China*
[b]*School of Computer Science, Chengdu University of Information Technology, Chengdu, China*

Abstract

Currently, existing efforts in Weakly Supervised Semantic Segmentation (WSSS) based on Convolutional Neural Networks (CNNs) have predominantly focused on enhancing the multi-label classification network stage, with limited attention given to the equally important downstream segmentation network. Furthermore, CNN-based local convolutions lack the ability to model the extensive inter-category dependencies. Therefore, this paper introduces a graph reasoning-based approach to enhance WSSS. The aim is to improve WSSS holistically by simultaneously enhancing both the multi-label classification and segmentation network stages. In the multi-label classification network segment, external knowledge is integrated, coupled with GCNs, to globally reason about inter-class dependencies. This encourages the network to uncover features in non-salient regions of images, thereby refining the completeness of generated pseudo-labels. In the segmentation network segment, the proposed Graph Reasoning Mapping (GRM) module is employed to leverage knowledge obtained from textual databases, facilitating contextual reasoning for class representation within image regions. This GRM module enhances feature representation in high-level semantics of the segmentation network's local convolutions, while dynamically learning semantic coherence for individual samples. Using solely

*Corresponding author.
Email addresses: JiaZhang@my.swjtu.edu.cn (Jia Zhang), bpeng@swjtu.edu.cn (Bo Peng), wuxi@cuit.edu.cn (Xi Wu)

image-level supervision, we have achieved state-of-the-art performance in WSSS on the PASCAL VOC 2012 and MS-COCO datasets. Extensive experimentation on both the multi-label classification and segmentation network stages underscores the effectiveness of the proposed graph reasoning approach for advancing WSSS. Our code is available at `https://github.com/JIA-ZHANG666/GRM_layer`.

Keywords: Weakly Supervised Semantic Segmentation, Convolutional Neural Networks, External Knowledge, Graph Reasoning

1. Introduction

The objective of semantic segmentation is to classify each pixel in an image into its corresponding semantic class. This forms the fundamental task for applications such as scene understanding Zhang et al. (2022), autonomous driving Treml et al. (2016), and medical imaging Havaei et al. (2017). However, the adoption of convolutional neural networks for such learning tasks requires a substantial amount of pixel-level annotated labels for supervised training. Acquiring these pixel-level labels demands significant human and computational resources. Therefore, some approaches have explored semi-supervised techniques Cao et al. (2022); Zhang et al. (2021c) and domain adaptation methods Tian & Zhu (2021); Zhou et al. (2022) to alleviate the reliance on labeled data. In recent years, weakly supervised semantic segmentation based on image-level labels has emerged as a solution to bypass the limitations of pixel-level annotations, gaining widespread attention Ahn et al. (2019); Zhang et al. (2020a). As illustrated in Figure 1, this weakly supervised approach initially entails training a multi-label classification network. Subsequently, by applying Class Activation Maps (CAM) to the trained classification model, specific seed regions for particular classes are inferred. These seeds are then expanded to generate Pseudo-Masks, which are employed as pseudo ground truth for the semantic segmentation network.

Currently, weakly supervised semantic segmentation utilizing image-level

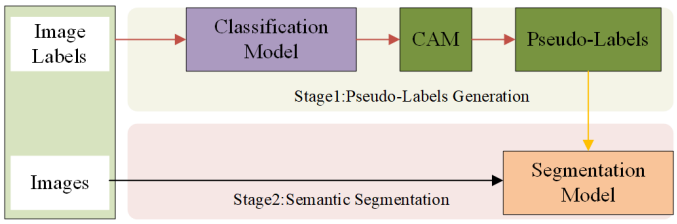

Figure 1: The prevailing pipeline for training weakly supervised semantic segmentation. Our contribution is to improve the classification model in the first phase, which is the foundation for better pseudo-masks. In the second stage, the segmentation model is improved to improve the final segmentation result.

labels relies on obtaining attribute mappings from a multi-label classification network. These methods are primarily based on Convolutional Neural Networks (CNN) models for weakly supervised semantic segmentation, which have demonstrated impressive results Lee et al. (2021a); Chen et al. (2022a). Moreover, establishing global contextual relationships between objects is crucial for the task of weakly supervised semantic segmentation (WSSS) in the absence of pixel-level annotations. However, these CNN-based methods tend to independently predict individual semantic labels, as seen in Figure 2, and often overlook the implicit semantic relationships between each label and pixel. Some existing efforts Zhang et al. (2020b) aim to implicitly model inter-class correlations through attention mechanisms, but these methods only construct local correlations. Although they establish relationships between participating regions in an image, they fail to leverage abundant background knowledge beyond a single image to infer global information between categories. Consequently, these approaches can result in inaccuracies such as misclassifications and mismatched label relationships. As a result, such methods often resort to time-consuming post-processing modules like Conditional Random Fields (CRF) Krähenbühl & Koltun (2011); Ji et al. (2020) to enforce spatial continuity in the output segmentation maps.

To address the aforementioned challenges and more effectively harness global contextual relationships between classes, we propose leveraging external semantic knowledge to enhance weakly supervised semantic segmentation. As de-

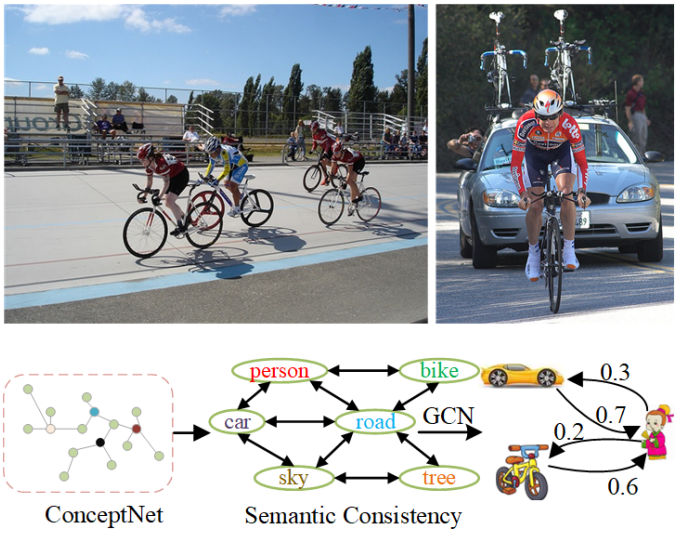

Figure 2: There are contextual semantic relationships among various categories in the scene graph. Firstly, the knowledge graph is designed from ConceptNet to initially obtain the semantic consistency of each category, and then further global relational reasoning is performed through GCN.

picted in Figure 2, context semantic relationships exist among various classes within a scene graph. Concretely, a semantic relationship graph constructed from external knowledge comprises textual entities such as "car," "person," and "bicycle" as vertices, interconnected by edges representing entity relationships. At a higher level of abstract semantics, the semantic relationship graph can extend category label nodes to include additional actions (e.g., "driving," "riding") while edges are derived from language descriptions. Integrating this high-level knowledge with human commonsense can guide the network to prune false interpretations based on the understanding of relationships between each category label, thereby promoting semantic coherence. In this work, we initially acquire semantic coherence for individual categories by designing a knowledge graph from a large-scale text corpus, ConceptNet Liu & Singh (2004). In this knowledge graph, each node corresponds to a category, and each edge signifies the relationship between two categories. The semantic coherence matrix obtained from this graph is used as the label correlation matrix for the Graph

Convolutional Network (GCN), guiding information propagation among GCN nodes for global relationship inference based on external semantic information. Subsequently, we integrate these relationships into the visual graph to enhance the network's discriminative capability. Inspired by the work of ML-GCN Chen et al. (2019c), in our multi-label classification network module, we introduce an additional classification loss to a set of interdependent classifiers derived from GCN. This augmentation strengthens the capability of the classification network to capture global relationships among distant regions, thus delving into features of less conspicuous regions within the image. Thereby promoting a more complete pseudo-label in the extended seed region. Moving to the semantic segmentation network segment, we propose a Graph Reasoning Mapping (GRM) module to leverage external semantic information and enhance contextual reasoning within the visual graph. Specifically, to complement local convolutions, we first feed the knowledge graph designed from extensive textual corpora into the GCN, engaging in global reasoning alongside visual feature maps. Subsequently, the evolved representation of the visual graph is mapped onto the local representation of the original feature map, thereby reinforcing the discriminative capacity of semantic segmentation. This process also serves to compensate for the limitations of pseudo-labels in comparison to ground truth labels. Through optimization in both the multi-label classification and segmentation networks, we achieve a comprehensive enhancement in the overall performance of weakly supervised semantic segmentation.

In the pseudo-label generation phase, we adopt the ReCAM Chen et al. (2022b) framework as our baseline and extensively validate our approach on the PASCAL VOC 2012 Everingham et al. (2010) and MS-COCO 2014 Lin et al. (2014) datasets. Notably, we achieve significant improvements in performance, particularly obtaining new state-of-the-art results on the validation sets of both datasets. Specifically, we attain impressive new mIoU scores of 70.2% and 46.1% on the validation sets of PASCAL VOC 2012 and MS-COCO 2014 respectively. Furthermore, the proposed GRM module can be seamlessly transferred to other WSSS tasks. This highlights the adaptability and effectiveness of our approach

beyond the initially tested datasets.

Our contributions can be summarized as follow:

- A new framework is proposed, which effectively combines the advantages of CNN and graph reasoning for weakly supervised semantic segmentation. The performance of WSSS is generally improved by the two stages of multi-label classification and semantic segmentation.
- The external knowledge graph is designed to guide the information dissemination between nodes in GCN, and applied in a multi-label classification network to obtain high-quality segmentation pseudo-labels.
- In the segmentation network part, a Graph Reasoning Mapping (GRM) module is proposed, which incorporates external knowledge to facilitate contextual reasoning on visual images. It provides a reference for the application of relational reasoning on visual feature maps using external knowledge.
- Extensive experiments on two general datasets show that our method has obvious advantages in weakly supervised semantic segmentation tasks, and the proposed GRM has strong generalization ability.

2. Related Work

In this section, we will briefly introduce the work related to weakly supervised semantic segmentation, graph convolutional networks, and graph inference learning on vision tasks. At the end of this section, we present the theoretical and practical implications of the proposed method and how our work differs from the previous ones.

2.1. Weakly Supervised Semantic Segmentation

Current approaches for weakly supervised semantic segmentation primarily focus on obtaining improved initial seeds to subsequently identify the regions occupied by target categories Wang et al. (2020b); Sun et al. (2020); Qin et al.

(2022). These seed regions provide a solid approximation of the area occupied by the target category, which is then expanded to recognize more instances of the target class. CMGC Meng et al. (2019) acquires initial local object priors through discriminative cues and utilizes local-to-global cues to segment object regions from these priors. The resulting segmented regions are then aggregated to form the semantic segmentation output. IRN Ahn et al. (2019) employs a relation network among pixels to evaluate class boundary maps. AdvCAM Lee et al. (2021a) employs an adversarial approach to perturb the image along pixel gradients, boosting classification scores and manipulating CAM to identify more object regions. CONTA Zhang et al. (2020a) adopts a causal intervention method to equitably incorporate all possible contexts into multi-label classification, generating improved CAM seed regions. ReCAM Chen et al. (2022b) leverages softmax cross-entropy loss (SCE) to reactivate more pixels in CAM. Building upon this, we introduce graph reasoning to establish global contextual relationships among objects.

2.2. Graph Neural Networks

Recent works have delved deep into various graph-based tasks, such as link prediction and node prediction, to construct Graph Convolutional Networks (GCNs) Rong et al. (2019); Xu et al. (2018); Li et al. (2019). DropEdge Rong et al. (2019) introduces sparsity into the network by randomly removing a certain proportion of edges from the graph during each input, mitigating the overfitting and over-smoothing issues associated with deep GCNs. Addressing the computational complexity of GNNs, which limits their practical applications, Li et al. Li et al. (2021a) propose models like RevGNN-Deep with 1001 layers and RevGNN-Wide with 448 layers. These models achieve memory consumption and parameter efficiency by incorporating balanced modeling, reversible connections, and weight sharing. Inspired by traditional CNNs, certain methods treat graph-based pooling operations as clustering assignment problems, extending the concept of local patches in regular grids to graph structures. DIFFPOOL Ying et al. (2018) extracts graph information through hierarchical pooling lay-

ers. Its novelty lies in assigning different nodes to various clusters via learned assignment matrices. This approach combines edge prediction regularization and entropy minimization to jointly optimize convolutional parameters. In the visual domain, some studies utilize GCNs to represent images as graphs, enhancing the performance of visual tasks through the integration of image-level features. Chen et al. Chen et al. (2020b) employ a graph attention network to capture latent semantic relationships among various target classes. Han et al. Han et al. (2022) segment input images into multiple patches, representing each patch as a node in the graph. Once the graph representation of the input image is constructed, the proposed ViG model facilitates information exchange among all nodes.

2.3. Graph reasoning learning for visual tasks

Current research related to Graph Neural Networks (GNNs) in the context of visual tasks mainly revolves around two objectives: (1) employing pure GNN structures, and (2) combining CNNs with GNNs. This paper primarily focuses on the latter, which is suitable for image classification and semantic segmentation tasks to enhance the long-range modeling capability of CNN-based visual features. In the image classification task, ML-GCN Chen et al. (2019c) constructs a directed graph in the label space and applies two GCN layers to label representations, generating a set of interdependent classifiers. This involves introducing label co-occurrence matrices and hyperparameters to modify the relationship matrix, thereby mitigating GCN overfitting. SSGRL Chen et al. (2019a) guides semantic feature propagation in different target regions through statistical label co-occurrence. MS-CMA You et al. (2020) introduces a cross-modal attention network to simultaneously explore discriminative regions and semantic dependencies in the label space. HSA Song et al. (2021) fuses label and scene-level feature word embeddings into category nodes, processing them via GCN to generate sample-adaptive global priors. These priors are then combined with point features to enhance the rationality of semantic predictions. MGTN Nguyen et al. (2021) decomposes image data into graph-structured data with

multiple subgraphs, achieving improved image classification by modeling relationships between various subgraphs in the image. DSGBI Xu et al. (2022a) initially fuses multi-modal high-level features through distant relationships in coordinate space. Subsequently, it clusters and allocates multi-modal features from a regular grid to vertices in feature space. By reasoning and enhancing relationships both within and between graphs, it extracts rich contextual information and semantically explores mutual benefits.

Additionally, to address the limitations of CNN-based semantic segmentation in inferring image context and establishing remote spatial dependencies, prior research has mostly extended architectures such as DeepLabv2 Chen et al. (2017a), DeepLabv3 Chen et al. (2017b), Pyramid Scene Parsing Network (PSPNet) Zhao et al. (2017), and self-attention mechanisms Zhang et al. (2020b, 2022) to explore either local or global contextual information within individual images. However, compared to such endeavors, GNN-based methods exhibit significant advantages in modeling global relationships and training efficiency. DGCNet Zhang et al. (2019) employs a dual GCN structure to model relationships between pixels in coordinate space and dependencies between channel dimensions in feature space. GloRe Chen et al. (2019b) constructs a latent space for global reasoning, projecting globally aggregated features from coordinate space onto the node domain and executing relational reasoning in a fully connected graph. Our graph reasoning module is built upon preliminary class relationship knowledge obtained from the ConceptNet textual repository. Through GCN, it further infers the correlation between semantic graphs and visual data, thereby evolving visual features and enhancing the model's context modeling capability.

2.4. The Difference with Other Method

We surveyed existing GCN-based weakly supervised semantic segmentation works. Zhou et al. Zhou et al. (2021) employ a set of input images as nodes and model relationships between pairs of images as edges, explicitly exploring semantic dependencies within image pairs to uncover rich semantic context.

WSGCN-I Pan et al. (2021) learns a 2-layer GCN for each training image by backpropagating Laplacian and entropy regularization losses. A2GNN Zhang et al. (2021a) introduces an affinity attention GNN, constructing semantic information interactions across remote regions in the graph via a designed affinity attention layer. However, these methods primarily optimize the upstream multi-label classification network responsible for generating pseudo-labels, neglecting the equally important segmentation network part. Moreover, the input graph relationships for these methods are mainly designed based on co-occurrence patterns of target classes, limiting GCN's ability to establish the quality of inter-label correlations during the initial inference stage. In contrast, our approach focuses on incorporating graph reasoning into both the classification network and the segmentation network shown in Figure 1. Additionally, our graph reasoning module is built upon preliminary class relationship knowledge obtained from the ConceptNet textual repository, which contains a vast amount of real-world background knowledge. Through GCN, we further infer the correlation between semantic graphs and visual data, evolving visual features, and enhancing the model's context modeling capability.

3. Approach

As described above, the weakly supervised semantic segmentation based on image-level labels must first train a multi-label classification network to obtain the pseudo-labels required by the segmentation network. Therefore, obtaining high-quality pseudo-labels largely determines the performance of the segmentation network. As shown in Figure 3, we therefore devote ourselves to exploring the acquisition of high-quality pseudo-labels upstream and the segmentation quality of the downstream segmentation network to improve the performance of weakly supervised semantic segmentation as a whole.

3.1. Graph Reasoning

Graph Convolutional Networks are deep trainable networks tailored for graph structures. These networks operate on graph features through graph convolution

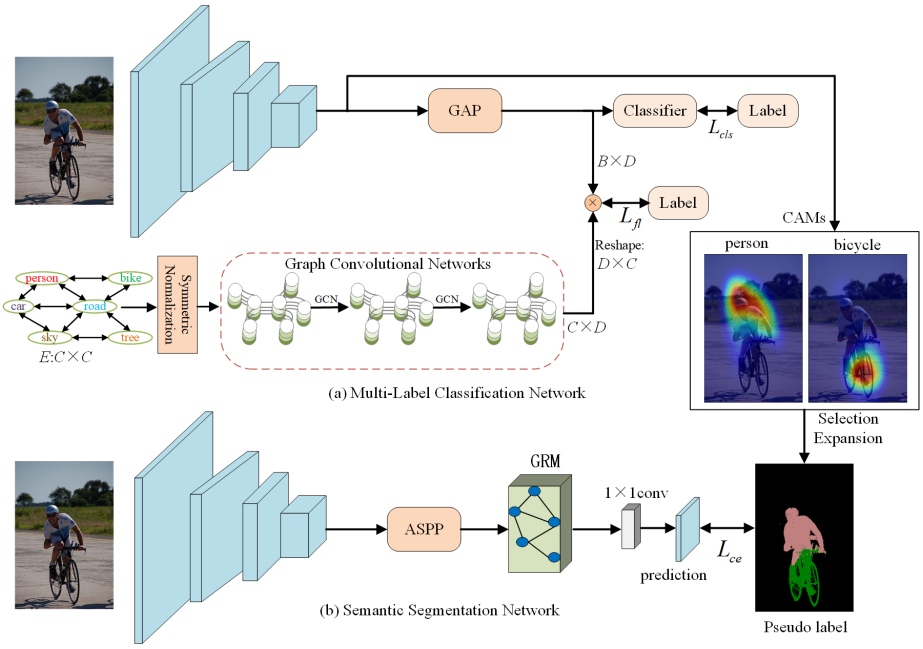

Figure 3: The overall flow chart of training WSSS, E is the acquired semantic relationship matrix, which is input into GCN for inference after symmetric normalization. GRM is our proposed graph reasoning mapping module.

operations, modifying node channels while establishing correlations between the new features of nodes and their adjacent nodes' prior features. Drawing from the insights of the semi-supervised classification method Kipf & Welling (2016), the graph $G = (V, E)$ is learned, where $E \in R^{C\times C}$ represents the semantic relationship matrix as edges, and $V \in R^{C\times D}$ represents vertices. Here, C denotes the number of nodes, which corresponds to the count of classes in the dataset excluding the background, and D stands for the feature dimensions of each node in the semantic graph. In this study, we utilize GloVe [28] word embeddings as the basis for node representation, setting $V \in R^{C\times K}$, where the initially acquired dimensionality of the word embeddings is $D = K = 300$. The associated matrix E is derived from ConceptNet, serving as an external knowledge graph source. For each GCN layer, the representation can be expressed as follows:

$$V^{l+1} = \sigma\left(EV^{l}W^{l}\right), \tag{1}$$

where σ is the activation function and $W^l \in R^{D\times D}$ is a trainable parameter.

In addition, inspired by GCN Kipf & Welling (2016), we normalize E, namely $Q^{-1/2}EQ^{-1/2}$, where Q is the diagonal node degree matrix of E. This symmetric normalization corresponds to taking the average of the features of neighboring nodes. Then the propagation rules of the GCN layer are updated as follows:

$$V^{l+1} = \sigma\left(\hat{Q}^{-1/2}\hat{E}\hat{Q}^{-1/2}V^l W^l\right), \tag{2}$$

where $\hat{E} = E + I$, I is the identity matrix, $\widehat{Q}_{ii} = \sum_j \widehat{E}_{ij}$.

3.2. Semantic Relation Matrix

Knowledge graphs can capture complex relationships among millions of entity classes Paulheim (2017), so it is beneficial to employ additional knowledge acquired from large-scale text corpora to establish semantic relationships between class labels. In order to obtain the semantic relationship graph E, we build it through the crowdsourcing knowledge graph ConceptNet.

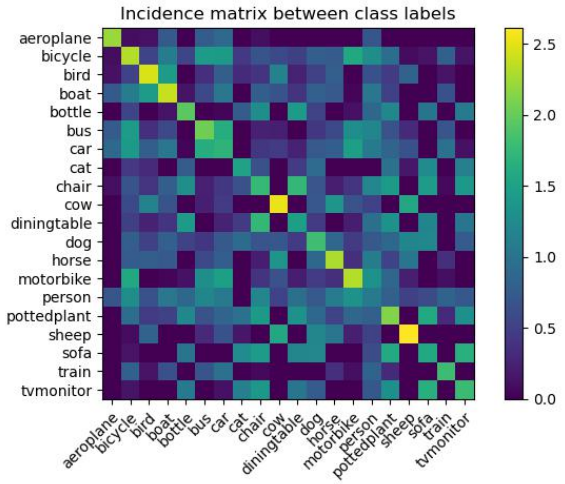

Figure 4: The relationship matrix built through the crowdsourcing knowledge map ConceptNet. Brighter blocks indicate stronger correlations between classes. Among them, the correlation of each class on the diagonal of the matrix is the strongest.

According to the method provided by the target detection work Fang et al. (2017), a set of predefined class labels $\mathrm{C} = \{\mathrm{c}_1, \mathrm{c}_2, \ldots, \mathrm{c}_n\}$ is given, and E is

expressed as a similar symmetric matrix of $C \times C$ to define the label c and c', $\forall\,(\mathrm{c}, \mathrm{c}') \in \mathrm{C}$. Therefore, the matrix E can model the relationship between different labels and prior knowledge. To construct C, random walks with restarts are employed to quantify semantic relevance on knowledge graphs. Let $\{\mathrm{v}_0, \mathrm{v}_1, \ldots, \mathrm{v}_t\}$ be represented as a random walk node sequence, and be represented by α as the probability of re-random walk each time, then the probability of reaching the class label c' within t steps starting from the class label c is $\mathrm{p}\left(\mathrm{v_t} = \mathrm{c}' \mid \mathrm{v}_0 = \mathrm{c}; \alpha\right)$. By computing the probabilities, denoted $R_{c,c'}$ as the final higher probability, where a greater probability means a higher correlation between two class labels. Specifically, the shorter path from node c to c' obtained by random walk, and thus the higher surface semantic correlation $E_{c,c'}$. So the matrix E can be calculated as follows:

$$\begin{aligned} R_{c,c'} &= \lim_{t\to\infty} p\left(r_t = c' \mid r_0 = c; \alpha\right), \\ E_{c,c'} &= E_{c',c} = \sqrt{R_{c,c'} R_{c',c}}. \end{aligned} \tag{3}$$

Figure 4 is the visualization result of our acquisition of the semantic relationship matrix. The brighter the block, the stronger the correlation between the classes. It can be seen from the figure that the same category on the diagonal of the matrix has the strongest correlation with itself. In addition, it can be seen from the bright squares in Figure 4 that there are correlations between "person" and "bicycle", "person" and "car", "person" and "hores", and "diningtable" and "chair" Stronger class pairs can establish a good connection. It is especially worth noting that the class pairs with indirect relationships such as "bottle" placed on "diningtable" and "cat" sitting on "sofa" have also been established in the relationship matrix.

3.3. Multi-label classification

As shown in Figure 3(a), we use ResNet-50 as the backbone network according to the baseline model ReCAM Chen et al. (2022b). The dimension of the feature map x output by the last layer of the network is 2048 dimensions, and

then global average pooling is performed on the feature map x. For the pooled features, we first pass through a classifier to get the prediction score x' of the category, and then do a traditional multi-label classification loss:

$$L_{\text{cls}} = -\frac{1}{C}\sum_{c=1}^{C} y_c \log\left(\sigma\left(x'_c\right)\right) + \left(1 - y_c\right)\log\left(1 - \sigma\left(x'_c\right)\right), \tag{4}$$

where C is the number of categories, y_c is the label corresponding to the c-th category, and σ is the activation function. On the other hand, inspired by ML-GCN Chen et al. (2019c), we adopt the above graph structure to capture the correlation dependencies between class labels. The node representation of the previous layer of the GCN layer is used as the input of the latter layer, and we follow the final output of the GCN node as a classifier with interdependence $V_c \in R^{C\times D}$ where D is the dimension of the node. Then multiply the obtained classifier with the last layer of feature map representation x after global average pooling and dimension transformation to get the prediction score, ie x. Finally, make an improved FocalLoss loss Lin et al. (2017) for the prediction and label to balance multi-class samples:

$$\begin{aligned} s_i &= e^{-\log(p_t)}, \\ L_{fl} &= -\left(1 - s_i\right)^{\gamma}\log\left(p_t\right), \end{aligned} \tag{5}$$

where p_t is the prediction confidence of the target class, and the value of focusing parameter γ is set here as 2.

Therefore, the overall loss of the multi-label classification network is:

$$L = L_{\text{cls}} + \lambda L_{fl}, \tag{6}$$

where λ is a hyperparameter, which we will conduct ablation studies in the experimental part.

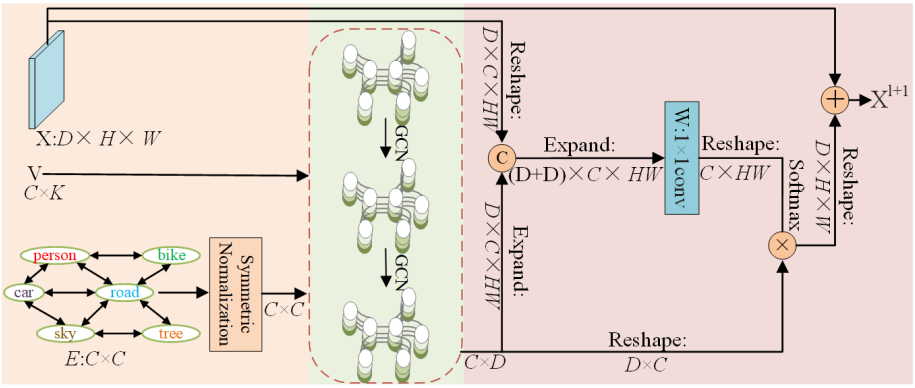

Figure 5: Implementation Details of the GRM Module with Convolutional Visual Features $X \in R^{D\times H\times W}$ as Input. ⓒ denotes concatenation, $\oplus$ signifies summation, and $\otimes$ indicates matrix multiplication. The initial dimensionality of word embeddings for V is set to $K = 300$. The weight matrix W is realized as a 1×1 convolution.

3.4. Semantic Segmentation

In the semantic segmentation network module in Figure 3(b) we use DeepLabV2 Chen et al. (2017a) whose backbone is ResNet-101. We input the feature map output by the last convolutional layer of the network into the Atrous Pyramid module (ASPP), and transform the final 2048-dimensional features to 256-dimensional. The 256-channel features output by ASPP are then fed into our proposed GRM module to capture visual context information.

The structure of the proposed GRM is shown in Figure 5. In the graph reasoning part, it is the same as the multi-label classification network. GCN uses the word embedding V and the relationship graph E we obtained through the ConceptNet library and normalizes them as input to obtain a semantic graph $V' \in R^{C\times D}$ with strong context dependencies. Therefore, the evolved global semantic graph representation can be used to improve the global feature representation ability of visual features. In order to find the most suitable mapping from the representation of each class node $v \in V'$ to each local visual feature $x_i \in X$. This is agnostic to learning the compatibility matrix H_v between class nodes and visual features. Inspired by the message propagation algorithm MPNNs Gilmer et al. (2017), we compute the weights $h_v \rightarrow x_i \in H_v$of the mapping by evaluating the compatibility of each class node v with each local

feature x_i:

$$h_{v \to x_i} = \frac{\exp\left([v, x_i]\, W\right)}{\sum_{x_i} \exp\left([v, x_i]\, W\right)}, \tag{7}$$

where $W \in R^{D \times D}$ is a trainable weight matrix obtained by a 1×1 convolution. The compatibility matrix $H_v \in R^{C \times HW}$ after softmax normalization, where H and W are the height and width of the feature map X, respectively. The evolutionary visual feature X^{l+1} obtained through global graph reasoning is used as the input of the next convolutional layer:

$$X^{l+1} = \sigma\left(H_v V^{l+1}\right) + X, \tag{8}$$

where σ is the ReLU activation function. Here we use residual links to augment the original features.

As shown in Figure 3(b), we finally adopt a 1×1 convolutional layer to predict the evolved feature map pixel by pixel, and perform cross-entropy loss calculation with the pseudo-label obtained by the multi-label classification network:

$$L_{ce} = -\sum_{c=1}^{c} \hat{y}_c \log\left(p_c\right), \tag{9}$$

where $\hat{y}_c$ is the pseudo-label for class c, and P_c is the predicted score for the corresponding class.

4. Experimental Setting

In this section, we qualitatively and quantitatively evaluate the effectiveness of the proposed method in terms of the performance of the model. Below we introduce the dataset, evaluation metrics, and experimental details. Ablation studies on baselines verify the superiority of the proposed graph inference method and compare it with state-of-the-art work.

4.1. Datasets

We evaluate the proposed method on two commonly used datasets, PASCAL VOC 2012 Everingham et al. (2010) and MS COCO 2014 Lin et al. (2014). PAS-

CAL VOC has 21 classes (one of which is the background class for semantic segmentation), and contains three subsets of training, validation and testing, and the corresponding images of each subset are 1464, 1449 and 1456 respectively. MS COCO has 81 classes (one of which is the background class), containing 80k images for training and 40k images for validation. Note that our training on both datasets uses only image-level class labels, which is challenging for weakly supervised semantic segmentation.

4.2. Evaluated Metric

Based on the training process of WSSS, we conduct evaluations separately for the classification and segmentation aspects. For the generation of pseudo-labels in the classification network, we compute the mIoU by producing pseudo-labels corresponding to the images in the training set and comparing them against their respective ground truths. Regarding the semantic segmentation network, we employ the pseudo-labels generated by the classification network as supervision for training the segmentation model. We then employ the trained segmentation model to predict masks on both the validation and test sets. Finally, the mIoU is computed by comparing these predicted masks with their corresponding ground truth.

4.3. Implementation Details

In our experimental setup, the classification network is akin to the baseline ReCAM Chen et al. (2022b), utilizing a ResNet50 backbone pre-trained on ImageNet as the basis for the multi-label classification network. The output stride is set at 16, and the final layer consists of a classifier with 20 channels. The parameter λ in Equation (6) is assigned a value of 0.0001. The initial learning rate for training is set to 0.1, while the learning rate for the graph convolutional layer is set at 0.01. Other settings remain consistent with those of the ReCAM baseline. For the semantic segmentation network, we employ a ResNet101 backbone pre-trained on ImageNet, which is then integrated into the DeepLabV2 architecture. Building upon this, we transform the 2048-dimensional feature from

the ASPP module to 256 dimensions. Subsequently, we incorporate the GRM (Graph Reasoning Module) layer for contextual relationship inference, followed by a 1×1 convolutional layer for per-pixel feature prediction. The initial learning rate is set to $2.5e^{-4}$, mirroring the settings outlined in Chen et al. (2017a). Furthermore, the learning rate for the GRM layer is established at 0.0001, and a weight decay of $5e^{-4}$ is applied.

5. Experimental results and analysis

In this section, we present a comprehensive performance comparison of the proposed method with other relevant state-of-the-art approaches on the PASCAL VOC 2012 and MS COCO 2014 datasets. We conduct an in-depth analysis of the obtained experimental results. In the ablation study, we delve into the incremental impact of each crucial component of the proposed method on the model's performance.

5.1. Comparison with State-of-the-arts

5.1.1. Improvements on localization maps

We initiated our evaluation by assessing the mIoU on class activation maps. Table 1 showcases a comparison between our proposed method and other prominent approaches on the PASCAL VOC 2012 training set. Following the approach of the baseline ReCAM Chen et al. (2022b), this study employed diverse weight acquisition for ReCAM seeds and employed the IRN for refinement. In contrast to the baseline ReCAM, our method demonstrates a 0.6% enhancement in seed accuracy and a 0.9% enhancement in pseudo-label accuracy after incorporating globally derived class relationships through graph convolution.

Figures 6 and 7 respectively illustrate the comparison of our method and the baseline's pseudo-label quality for foreground classes' localization and generation on the PASCAL VOC 2012 training set. From these figures, the efficacy of our approach in capturing entire semantic regions across diverse scenes is evident. Particularly noteworthy is the effective discrimination achieved by our

Table 1: Evaluation of initial seeds (Seed) and corresponding pseudo-labels (Pseudo) in terms of mIoU (%) on the PASCAL VOC training set.

Methods	Pub.	Seed	Pseudo
IRN Ahn et al. (2019)	CVPR19	48.8	66.3
CONTA Zhang et al. (2020a)	NIPS20	48.8	67.9
MCTformer Xu et al. (2022b)	CVPR22	61.7	69.1
AMR Qin et al. (2022)	AAAI22	56.8	69.7
AdvCAM Lee et al. (2021a)	CVPR21	55.6	69.9
CLIMS Xie et al. (2022)	CVPR22	56.6	70.5
LPCAM Chen & Sun (2023)	CVPR23	54.9	71.2
ReCAM Chen et al. (2022b)	CVPR22	54.8	70.5
Ours		55.4	**71.4**

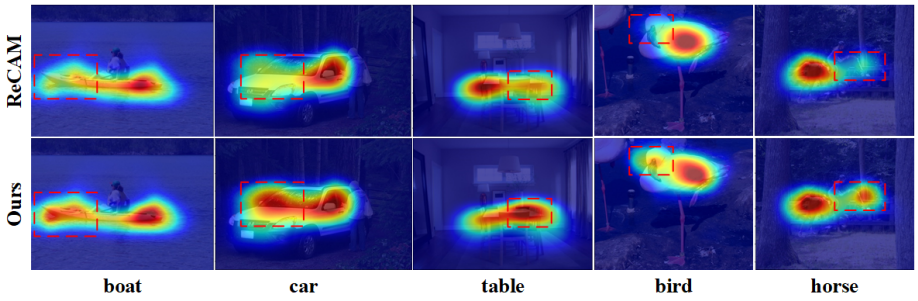

Figure 6: Localization of foreground classes compared to baseline models on the PASCAL VOC 2012 training set. ReCAM is the baseline method for comparison.

method between categories with global semantic correlations, such as distinguishing a helmet worn by a person from a motorcycle, which possess global semantic association, as showcased in the figures. Additionally, for closely related categories like "bottle" and "dining table," our network exhibits a higher focus on "bottle" compared to the baseline, as evidenced by the class activation maps. The generated pseudo-labels also demonstrate reduced class ambiguity between "bottle" and "dining table," leading to enhanced category discrimination. This outcome is attributed to the external knowledge integration from textual and conceptual sources through ConceptNet, coupled with semantic context reasoning conducted by the GCN, thereby emphasizing the role of semantic context primarily guided by object class classification knowledge.

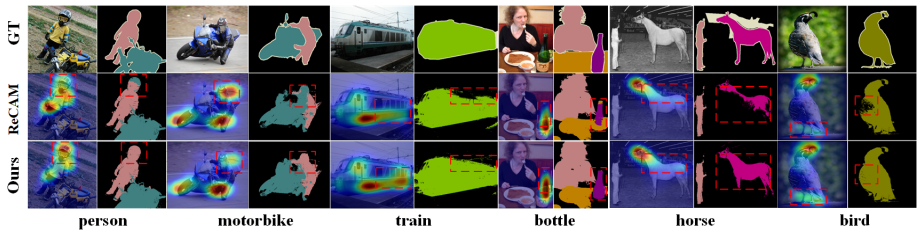

Figure 7: Visual comparison of CAM and pseudo-labels generated by baseline models on the PASCAL VOC 2012 training set. The first row is the original image and its corresponding ground truth, the second row ReCAM is the baseline method, and the third row is our result.

5.1.2. Improvements on segmentation

Table 2 presents the mIoU achieved by our proposed method in the classification network and after integrating the GRM module into the segmentation network. We employ the pseudo-labels generated by the aforementioned classification network to train a fully supervised model. Subsequently, we compare the results on the PASCAL VOC 2012 validation and test sets with state-of-the-art methods. Through methods that solely employ image-level labels, our approach achieves mIoU scores of 69.2% and 69.4% on the validation and test sets, respectively. Moreover, following the integration of our proposed GRM module into the segmentation network, the segmentation accuracy on the validation and test sets rises to 70.2% and 70.3%, respectively, demonstrating an enhancement of 1.7% and 1.9% compared to ReCAM. This validates the effectiveness of employing explicit graph reasoning beyond local convolutions for large-scale pixel-wise classification recognition.

Figure 8 displays the qualitative segmentation outcomes of our method on the PASCAL VOC 2012 validation set. Benefitting from joint reasoning of correlated classes on the class hierarchy graph, our approach successfully combines high-level semantic constraints of the classification task into pixel recognition within visual feature maps. Notably, integrating dense pixel relationships with prior knowledge is a challenging endeavor in itself. Our proposed GRM module remarkably improves results through a single inference step. As compared to ReCAM, our segmentation outcomes exhibit superior performance not only in

Table 2: Performance comparison of mIoU (%) of WSSS method on PASCAL VOC 2012 val and test set using different split backbones.Sup.: supervision. I: image-level ground-truth labels. S: off-the-shelf saliency maps.

Method	Pub.	Sup.	Backbone	Val	Test
MCIS Sun et al. (2020)	ECCV20	I+S	ResNet-101	66.2	66.9
ICD Fan et al. (2020)	CVPR20	I+S	ResNet101	67.8	68.0
G-WSSS Li et al. (2021b)	AAAI21	I+S	ResNet101	68.2	68.5
AuxSegNet Xu et al. (2021)	ICCV21	I+S	WResNet-38	69.0	68.6
NSROM Yao et al. (2021)	CVPR21	I+S	ResNet101	70.4	70.2
EDAM Wu et al. (2021)	CVPR21	I+S	ResNet-101	70.9	70.6
L2G Jiang et al. (2022)	CVPR22	I+S	ResNet-101	72.1	71.7
IRN Ahn et al. (2019)	CVPR19	I	ResNet-50	63.5	64.8
MCIS Sun et al. (2020)	ECCV20	I	ResNet101	66.2	66.9
CONTA Zhang et al. (2020a)	NIPS20	I	ResNet101	66.1	66.7
A2GNN Zhang et al. (2021a)	TPAMI21	I	ResNet101	66.8	67.4
ECS Sun et al. (2021)	ICCV21	I	ResNet38	66.6	67.6
CSE Kweon et al. (2021)	ICCV21	I	ResNet38	68.4	68.2
CPN Zhang et al. (2021b)	ICCV21	I	ResNet38	67.8	68.5
AdvCAM Lee et al. (2021a)	CVPR21	I	ResNet101	68.1	68.0
LPCAM Chen & Sun (2023)	CVPR23	I	ResNet101	68.6	68.7
AMR Qin et al. (2022)	AAAI22	I	ResNet101	68.8	69.1
SIPE Chen et al. (2022a)	CVPR22	I	ResNet101	68.8	69.7
ReCAM Chen et al. (2022b)	CVPR22	I	ResNet101	68.5	68.4
Ours		I	ResNet101	69.2	69.4
Ours+GRM		I	ResNet101	**70.2**	**70.3**

related class scenarios such as "person" riding "bicycle" and "person" riding "horse," but also in the intricate segmentation recognition of individual categories' contours like "sheep" and "bird."

To further assess the performance of our method, Table 3 presents the segmentation results on the MS COCO 2014 dataset. Achieving high-quality pseudo-labels solely using our graph reasoning on the validation set yields a 45.4%. Upon integrating the proposed GRM module into the segmentation network, the segmentation accuracy rises to 46.1%, which is 1.1% higher than ReCAM. Additionally, a comparison within Table 3 reveals that the performance attained through methods employing additional saliency maps fares worse than methods utilizing solely image-level labels for segmentation. This indicates the

Figure 8: Qualitative segmentation results comparison with baseline ReCAM on PASCAL VOC 2012 validation set. The first and second lines are the original image and its corresponding ground truth respectively, the third line ReCAM is the baseline segmentation result, the fourth line is the segmentation result we only use graph reasoning in the classification network, and the last line is the segmentation network at the same time Segmentation results after using the GRM module.

limitations of enhancing performance by introducing pre-trained saliency models. Consequently, such models exhibit subpar results on the challenging MS COCO 2014 dataset.

5.2. Ablation Studies

5.2.1. Importance of the Weights of the L_{fl}-loss

To investigate the necessity of the improved L_{fl} losses on balancing categories, we trained multi-label classification networks with different L_{fl} loss weights. The value of λ is shown in Table 4. It is worth noting that the value of λ here is only part of the experiments we conducted near the best results.In the experiment, we found that higher weight does not bring more performance improvement, and a smaller λ value will make the L_{fl} loss only occupy a smaller proportion in the overall segmentation loss, so that the L_{fl} loss will return to The gradient contribution passed is also very small, so it does not have much effect on difficult-to-segment samples.

Table 3: Performance comparison of mIoU (%) of WSSS methods on the MS COCO validation set using different split backbones.

Method	Pub.	Sup.	Backbone	Val
DSRG Huang et al. (2018)	CVPR18	I+S	VGG16	26.0
G-WSSS Li et al. (2021b)	AAAI21	I+S	ResNet101	28.4
AuxSegNet Xu et al. (2021)	ICCV21	I+S	ResNet38	33.9
EPS Lee et al. (2021b)	CVPR21	I+S	ResNet101	35.7
IRN Ahn et al. (2019)	CVPR19	I	ResNet50	32.6
IAL Wang et al. (2020a)	IJCV20	I	VGG16	27.7
CONTA Zhang et al. (2020a)	NIPS20	I	ResNet101	33.4
CSE Kweon et al. (2021)	ICCV21	I	ResNet38	52.6
SIPE Chen et al. (2022a)	CVPR22	I	ResNet101	40.6
MCTformer Xu et al. (2022b)	CVPR22	I	ResNet38	42.0
LPCAM Chen & Sun (2023)	CVPR23	I	ResNet101	44.5
ReCAM Chen et al. (2022b)	CVPR22	I	ResNet101	45.0
Ours		I	ResNet101	45.4
Ours+GRM		I	ResNet101	**46.1**

Table 4: Effect of hyperparameter λ on seed generation.

λ	0.0002	0.00015	0.0001	0.000095	0.00009
$mIoU$	54.5	55.0	**55.4**	55.1	54.8

The parameter γ smoothly adjusts the ratio of easy-to-classify sample weights. We discuss in Figure 9 the degree of attention to hard-to-segment sample classes for different values of γ in the case of $\lambda = 0.0001$. As we all know, when the value of γ is 0, the L_{fl} loss will degenerate into cross-entropy loss, so the value of $\gamma = 0$ is useless to us. The larger the value of γ, the greater the effect of the modulation factor, so that samples with higher accuracy are attenuated more, and samples with lower accuracy are attenuated less, so the loss weight for difficult-to-segment samples is greater. It is found through experiments that taking γ as 2 is the best for our method.

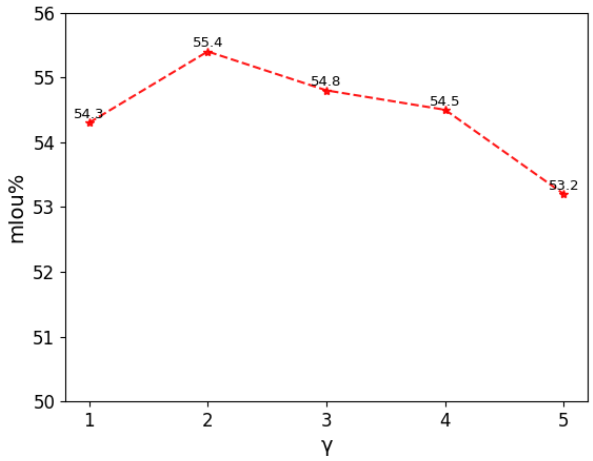

Figure 9: Effects of different values of γ on seed generation on the PASCAL VOC dataset.

Table 5: Deploying GRM after different residual layers.

ConvBlock	layer-1	layer-2	layer-3	layer-4	ASPP
mIoU	69.3	69.5	68.9	69.2	**70.2**

5.2.2. Which ConvBlock to add GRM layer?

Table 5 compares the variant results after adding a single GRM module to different residual blocks of ResNet-101. Compared to Table 1, when GRM is not used, the result on the verification set is 69.2%, and when the GRM layer is added after the residual block layer-1 and layer-2, there will be a slight improvement, which shows that our GRM is for Boosting visual features can help. But it is worth noting that the segmentation performance decreased slightly after the introduction of GRM after the residual block layer-3 and layer-4, but it improved significantly when the channel dimension was reduced to 256 after ASPP. We posit a plausible interpretation that ASPP facilitates encoding of more sophisticated abstract semantic features, rendering it more apt for global contextual graph reasoning. Furthermore, as convolutional networks deepen, the output channels of layer-3 and layer-4 expand to 1024 and 2048 dimensions,

respectively. Consequently, the graph convolutional outputs of the GRM module also increase to 1024 and 2048 dimensions. This augmentation in large-channel semantic relationships becomes unfavorable for amalgamating with visual features due to mapping complexities.

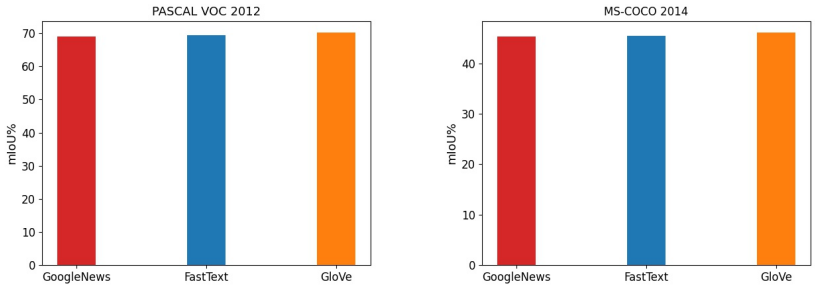

Figure 10: The effect of using different semantic relation matrices on establishing label contextual relations on PASCAL VOC 2012 and MS-COCO datasets.

5.2.3. GCN with different word embedding nodes

We use the word embedding GloVe Pennington et al. (2014) as the node input of GCN by default. Figure 10 illustrates the robustness of our proposed method with different word embedding nodes and thereby observes the impact of using distinct word embeddings as GCN inputs on establishing label contextual relationships. We perform comparative experiments by employing two popular word embeddings, GoogleNews Mikolov et al. (2013) and FastText Joulin et al. (2016), in contrast to GloVe Pennington et al. (2014). Based on the segmentation outcomes on PASCAL VOC 2012 and MS-COCO 2014 as depicted in Figure 10, it is discernible that various word embeddings do not induce significant fluctuations in the final results. This observation suggests the high generality of the introduced GRM module. Regardless of the employed word embedding matrix, the proposed GRM consistently succeeds in capturing the overarching semantic connections among labels and seamlessly integrating with visual features. It is worth noting that the application of the robust relationship matrix, ConceptNet, as the matrix of label correlations leads to improved performance. Our analysis indicates that the relationship matrix acquired from extensive textual

corpora inherently preserves the semantic topological relationships among labels. Hence, for semantically related class labels, their embeddings tend to be in close proximity within the embedding space. Furthermore, our model adeptly exploits these implicit dependency relationships to a full extent.

5.2.4. Comparison With Each Classification

Table 6 presents the accuracy of our approach for various categories on the validation set of PASCAL VOC 2012. A comparison with several recent methods reveals the advantages of our results across most categories. Moreover, superior performance is demonstrated in categories characterized by global semantic relationships, such as instances where "person" rides a "boat," "person" watches "tv," and associations between "bottle" and "table," among others. Furthermore, our approach exhibits a notable advantage in handling certain challenging samples.

Table 6: Comparison of per-category performance on PASCAL VOC 2012 validation set.

Models	*bkg*	*aero*	*bike*	*bird*	*boat*	*bottle*	*bus*	*car*	*cat*	*chair*	*cow*	*table*	*dog*	*horse*	*mbk*	*prsn*	*plnt*	*sheep*	*sofa*	*train*	*tv*	*mIoU*
AdvErasing Wei et al. (2017)	83.4	71.1	30.5	72.9	41.6	55.9	63.1	60.2	74.0	18.0	66.5	32.4	71.7	56.3	64.8	52.4	37.4	69.1	31.4	58.9	43.9	55.0
AffinityNet Ahn & Kwak (2018)	88.2	68.2	30.6	81.1	49.6	61.0	77.8	66.1	75.1	29.0	66.0	40.2	80.4	62.0	70.4	73.7	42.5	70.7	42.6	**68.1**	51.6	61.7
SEAM Wang et al. (2018)	88.8	68.5	33.3	85.7	40.4	67.3	78.9	76.3	81.9	29.1	75.5	48.1	79.9	73.8	71.4	75.2	48.9	79.8	40.9	58.2	53.0	64.5
SSDD Shimoda & Yanai (2019)	89.0	62.5	28.9	83.7	52.9	59.5	77.6	73.7	87.0	34.0	83.7	47.6	84.1	77.0	73.9	69.6	29.8	84.0	43.2	68.0	53.4	64.9
BES Chen et al. (2020a)	88.9	74.1	29.8	81.3	53.3	69.9	89.4	79.8	84.2	27.9	76.9	46.6	78.8	75.9	72.2	70.4	50.8	79.4	39.9	65.3	44.8	65.7
IRN Ahn et al. (2019)	90.2	75.8	32.5	76.5	49.6	65.9	82.6	76.2	82.7	31.8	77.5	41.8	79.4	75.0	81.2	75.2	47.9	81.1	**51.5**	62.5	59.1	66.5
ECS Sun et al. (2021)	89.8	68.4	33.4	85.6	48.6	72.2	87.4	78.1	86.8	33.0	77.5	41.6	81.7	76.9	75.4	75.6	46.2	80.7	43.9	59.8	56.3	66.6
G-WSSS Li et al. (2021b)	90.2	**82.9**	**35.1**	86.8	59.4	70.6	82.5	78.1	87.4	30.1	79.4	45.9	83.1	83.4	75.7	73.4	48.1	**89.3**	42.7	60.4	52.3	68.4
WSGCN-I Pan et al. (2021)	**91.0**	79.8	33.8	78.2	50.9	65.7	86.8	79.3	86.0	27.4	75.2	**48.9**	83.4	76.2	**82.7**	74.4	**64.3**	86.0	51.0	64.2	58.6	68.8
Ours	90.5	70.3	32.5	84.5	56.9	72.0	**90.1**	80.4	87.8	30.9	82.6	48.0	81.7	83.2	74.4	**78.1**	51.7	82.6	46.3	64.9	59.6	69.0
Ours+GRM	90.9	70.2	33.2	**87.0**	**62.3**	**73.1**	89.9	**81.7**	**89.0**	**33.2**	**83.7**	47.0	**84.9**	**83.7**	74.3	**78.1**	53.1	83.7	47.9	65.4	**61.2**	**70.2**

6. Conclusion

The lack of utilization of surrounding information is a key problem in classical weakly supervised semantic segmentation. In this paper, the multi-label classification network first performs global class reasoning on the external knowledge relationship matrix obtained from ConceptNet through GCN to capture the dependency on the category, so as to obtain high-quality pseudo-labels. Additionally, we design a GRM module for the segmentation network to facilitate contextual reasoning on visual graphs by incorporating semantic knowledge. From the experimental results, it proves the effectiveness of our proposed

method. And we hope to further explore the more detailed fusion of semantic relationship knowledge and visual images in the next step.

Acknowledgements

This work was supported by Natural Science Foundation of Sichuan China (No. 2022NSFSC0502), National Science Foundation of China (No. 42075142) and Key Research and Development Program of Sichuan Province(No. 2023YFG0125).

Conflict of Interest Statement

We declare that we have no financial and personal relationships with other people or organizations that can inappropriately influence our work. There is no professional or other personal interest of any nature or kind in any product, service and/or company that could be construed as influencing the position presented in, or the review of, the manuscript entitled.

References

Ahn, J., Cho, S., & Kwak, S. (2019). Weakly supervised learning of instance segmentation with inter-pixel relations. In *Proceedings of the IEEE/CVF conference on computer vision and pattern recognition* (pp. 2209–2218).

Ahn, J., & Kwak, S. (2018). Learning pixel-level semantic affinity with image-level supervision for weakly supervised semantic segmentation. In *Proceedings of the IEEE conference on computer vision and pattern recognition* (pp. 4981–4990).

Cao, C., Lin, T., He, D., Li, F., Yue, H., Yang, J., & Ding, E. (2022). Adversarial dual-student with differentiable spatial warping for semi-supervised semantic segmentation. *IEEE Transactions on Circuits and Systems for Video Technology*, .

Chen, L., Wu, W., Fu, C., Han, X., & Zhang, Y. (2020a). Weakly supervised semantic segmentation with boundary exploration. In *Computer Vision–ECCV 2020: 16th European Conference, Glasgow, UK, August 23–28, 2020, Proceedings, Part XXVI 16* (pp. 347–362). Springer.

Chen, L.-C., Papandreou, G., Kokkinos, I., Murphy, K., & Yuille, A. L. (2017a). Deeplab: Semantic image segmentation with deep convolutional nets, atrous convolution, and fully connected crfs. *IEEE transactions on pattern analysis and machine intelligence*, *40*, 834–848.

Chen, L.-C., Papandreou, G., Schroff, F., & Adam, H. (2017b). Rethinking atrous convolution for semantic image segmentation. *arXiv preprint arXiv:1706.05587*, .

Chen, Q., Yang, L., Lai, J.-H., & Xie, X. (2022a). Self-supervised image-specific prototype exploration for weakly supervised semantic segmentation. In *Proceedings of the IEEE/CVF Conference on Computer Vision and Pattern Recognition* (pp. 4288–4298).

Chen, S., Li, Z., & Tang, Z. (2020b). Relation r-cnn: A graph based relation-aware network for object detection. *IEEE Signal Processing Letters*, *27*, 1680–1684.

Chen, T., Xu, M., Hui, X., Wu, H., & Lin, L. (2019a). Learning semantic-specific graph representation for multi-label image recognition. In *Proceedings of the IEEE/CVF international conference on computer vision* (pp. 522–531).

Chen, Y., Rohrbach, M., Yan, Z., Shuicheng, Y., Feng, J., & Kalantidis, Y. (2019b). Graph-based global reasoning networks. In *Proceedings of the IEEE/CVF Conference on Computer Vision and Pattern Recognition* (pp. 433–442).

Chen, Z., & Sun, Q. (2023). Extracting class activation maps from non-discriminative features as well. In *Proceedings of the IEEE/CVF Conference on Computer Vision and Pattern Recognition* (pp. 3135–3144).

Chen, Z., Wang, T., Wu, X., Hua, X.-S., Zhang, H., & Sun, Q. (2022b). Class re-activation maps for weakly-supervised semantic segmentation. In *Proceedings of the IEEE/CVF Conference on Computer Vision and Pattern Recognition* (pp. 969–978).

Chen, Z.-M., Wei, X.-S., Wang, P., & Guo, Y. (2019c). Multi-label image recognition with graph convolutional networks. In *Proceedings of the IEEE/CVF conference on computer vision and pattern recognition* (pp. 5177–5186).

Everingham, M., Van Gool, L., Williams, C. K., Winn, J., & Zisserman, A. (2010). The pascal visual object classes (voc) challenge. *International journal of computer vision*, *88*, 303–338.

Fan, J., Zhang, Z., Song, C., & Tan, T. (2020). Learning integral objects with intra-class discriminator for weakly-supervised semantic segmentation. In *Proceedings of the IEEE/CVF Conference on Computer Vision and Pattern Recognition* (pp. 4283–4292).

Fang, Y., Kuan, K., Lin, J., Tan, C., & Chandrasekhar, V. (2017). Object detection meets knowledge graphs. International Joint Conferences on Artificial Intelligence.

Gilmer, J., Schoenholz, S. S., Riley, P. F., Vinyals, O., & Dahl, G. E. (2017). Neural message passing for quantum chemistry. In *International conference on machine learning* (pp. 1263–1272). PMLR.

Han, K., Wang, Y., Guo, J., Tang, Y., & Wu, E. (2022). Vision gnn: An image is worth graph of nodes. *arXiv preprint arXiv:2206.00272*, .

Havaei, M., Davy, A., Warde-Farley, D., Biard, A., Courville, A., Bengio, Y., Pal, C., Jodoin, P.-M., & Larochelle, H. (2017). Brain tumor segmentation with deep neural networks. *Medical image analysis*, *35*, 18–31.

Huang, Z., Wang, X., Wang, J., Liu, W., & Wang, J. (2018). Weakly-supervised semantic segmentation network with deep seeded region growing. In *Proceedings of the IEEE conference on computer vision and pattern recognition* (pp. 7014–7023).

Ji, J., Shi, R., Li, S., Chen, P., & Miao, Q. (2020). Encoder-decoder with cascaded crfs for semantic segmentation. *IEEE Transactions on Circuits and Systems for Video Technology*, *31*, 1926–1938.

Jiang, P.-T., Yang, Y., Hou, Q., & Wei, Y. (2022). L2g: A simple local-to-global knowledge transfer framework for weakly supervised semantic segmentation. In *Proceedings of the IEEE/CVF Conference on Computer Vision and Pattern Recognition* (pp. 16886–16896).

Joulin, A., Grave, E., Bojanowski, P., Douze, M., Jégou, H., & Mikolov, T. (2016). Fasttext. zip: Compressing text classification models. *arXiv preprint arXiv:1612.03651*, .

Kipf, T. N., & Welling, M. (2016). Semi-supervised classification with graph convolutional networks. *arXiv preprint arXiv:1609.02907*, .

Krähenbühl, P., & Koltun, V. (2011). Efficient inference in fully connected crfs with gaussian edge potentials. *Advances in neural information processing systems*, *24*.

Kweon, H., Yoon, S.-H., Kim, H., Park, D., & Yoon, K.-J. (2021). Unlocking the potential of ordinary classifier: Class-specific adversarial erasing framework for weakly supervised semantic segmentation. In *Proceedings of the IEEE/CVF International Conference on Computer Vision* (pp. 6994–7003).

Lee, J., Kim, E., & Yoon, S. (2021a). Anti-adversarially manipulated attributions for weakly and semi-supervised semantic segmentation. In *Proceedings of the IEEE/CVF Conference on Computer Vision and Pattern Recognition* (pp. 4071–4080).

Lee, S., Lee, M., Lee, J., & Shim, H. (2021b). Railroad is not a train: Saliency as pseudo-pixel supervision for weakly supervised semantic segmentation. In *Proceedings of the IEEE/CVF conference on computer vision and pattern recognition* (pp. 5495–5505).

Li, G., Müller, M., Ghanem, B., & Koltun, V. (2021a). Training graph neural networks with 1000 layers. In *International conference on machine learning* (pp. 6437–6449). PMLR.

Li, G., Muller, M., Thabet, A., & Ghanem, B. (2019). Deepgcns: Can gcns go as deep as cnns? In *Proceedings of the IEEE/CVF international conference on computer vision* (pp. 9267–9276).

Li, X., Zhou, T., Li, J., Zhou, Y., & Zhang, Z. (2021b). Group-wise semantic mining for weakly supervised semantic segmentation. In *Proceedings of the AAAI Conference on Artificial Intelligence* (pp. 1984–1992). volume 35.

Lin, T.-Y., Goyal, P., Girshick, R., He, K., & Dollár, P. (2017). Focal loss for dense object detection. In *Proceedings of the IEEE international conference on computer vision* (pp. 2980–2988).

Lin, T.-Y., Maire, M., Belongie, S., Hays, J., Perona, P., Ramanan, D., Dollár, P., & Zitnick, C. L. (2014). Microsoft coco: Common objects in context. In *Computer Vision–ECCV 2014: 13th European Conference, Zurich, Switzerland, September 6-12, 2014, Proceedings, Part V 13* (pp. 740–755). Springer.

Liu, H., & Singh, P. (2004). Conceptnet—a practical commonsense reasoning tool-kit. *BT technology journal*, *22*, 211–226.

Meng, F., Luo, K., Li, H., Wu, Q., & Xu, X. (2019). Weakly supervised semantic segmentation by a class-level multiple group cosegmentation and foreground fusion strategy. *IEEE Transactions on Circuits and Systems for Video Technology*, *30*, 4823–4836.

Mikolov, T., Chen, K., Corrado, G., & Dean, J. (2013). Efficient estimation of word representations in vector space. *arXiv preprint arXiv:1301.3781*, .

Nguyen, H. D., Vu, X.-S., & Le, D.-T. (2021). Modular graph transformer networks for multi-label image classification. In *Proceedings of the AAAI Conference on Artificial Intelligence* (pp. 9092–9100). volume 35.

Pan, S.-Y., Lu, C.-Y., Lee, S.-P., & Peng, W.-H. (2021). Weakly-supervised image semantic segmentation using graph convolutional networks. In *2021 IEEE International Conference on Multimedia and Expo (ICME)* (pp. 1–6). IEEE.

Paulheim, H. (2017). Knowledge graph refinement: A survey of approaches and evaluation methods. *Semantic web*, *8*, 489–508.

Pennington, J., Socher, R., & Manning, C. D. (2014). Glove: Global vectors for word representation. In *Proceedings of the 2014 conference on empirical methods in natural language processing (EMNLP)* (pp. 1532–1543).

Qin, J., Wu, J., Xiao, X., Li, L., & Wang, X. (2022). Activation modulation and recalibration scheme for weakly supervised semantic segmentation. In *Proceedings of the AAAI Conference on Artificial Intelligence* (pp. 2117–2125). volume 36.

Rong, Y., Huang, W., Xu, T., & Huang, J. (2019). Dropedge: Towards deep graph convolutional networks on node classification. *arXiv preprint arXiv:1907.10903*, .

Shimoda, W., & Yanai, K. (2019). Self-supervised difference detection for weakly-supervised semantic segmentation. In *Proceedings of the IEEE/CVF International Conference on Computer Vision* (pp. 5208–5217).

Song, Z., Zhao, L., & Zhou, J. (2021). Learning hybrid semantic affinity for point cloud segmentation. *IEEE Transactions on Circuits and Systems for Video Technology*, *32*, 4599–4612.

Sun, G., Wang, W., Dai, J., & Van Gool, L. (2020). Mining cross-image semantics for weakly supervised semantic segmentation. In *Computer Vision–ECCV 2020: 16th European Conference, Glasgow, UK, August 23–28, 2020, Proceedings, Part II 16* (pp. 347–365). Springer.

Sun, K., Shi, H., Zhang, Z., & Huang, Y. (2021). Ecs-net: Improving weakly supervised semantic segmentation by using connections between class activation maps. In *Proceedings of the IEEE/CVF International Conference on Computer Vision* (pp. 7283–7292).

Tian, Y., & Zhu, S. (2021). Partial domain adaptation on semantic segmentation. *IEEE Transactions on Circuits and Systems for Video Technology*, *32*, 3798–3809.

Treml, M., Arjona-Medina, J., Unterthiner, T., Durgesh, R., Friedmann, F., Schuberth, P., Mayr, A., Heusel, M., Hofmarcher, M., Widrich, M. et al. (2016). Speeding up semantic segmentation for autonomous driving, .

Wang, X., Liu, S., Ma, H., & Yang, M.-H. (2020a). Weakly-supervised semantic segmentation by iterative affinity learning. *International Journal of Computer Vision*, *128*, 1736–1749.

Wang, X., You, S., Li, X., & Ma, H. (2018). Weakly-supervised semantic segmentation by iteratively mining common object features. In *Proceedings of the IEEE conference on computer vision and pattern recognition* (pp. 1354–1362).

Wang, Y., Zhang, J., Kan, M., Shan, S., & Chen, X. (2020b). Self-supervised equivariant attention mechanism for weakly supervised semantic segmentation. In *Proceedings of the IEEE/CVF Conference on Computer Vision and Pattern Recognition* (pp. 12275–12284).

Wei, Y., Feng, J., Liang, X., Cheng, M.-M., Zhao, Y., & Yan, S. (2017). Object region mining with adversarial erasing: A simple classification to semantic segmentation approach. In *Proceedings of the IEEE conference on computer vision and pattern recognition* (pp. 1568–1576).

Wu, T., Huang, J., Gao, G., Wei, X., Wei, X., Luo, X., & Liu, C. H. (2021). Embedded discriminative attention mechanism for weakly supervised semantic segmentation. In *Proceedings of the IEEE/CVF Conference on Computer Vision and Pattern Recognition* (pp. 16765–16774).

Xie, J., Hou, X., Ye, K., & Shen, L. (2022). Cross language image matching for weakly supervised semantic segmentation. *arXiv preprint arXiv:2203.02668*, .

Xu, C., Li, Q., Jiang, X., Yu, D., & Zhou, Y. (2022a). Dual-space graph-based interaction network for rgb-thermal semantic segmentation in electric power scene. *IEEE Transactions on Circuits and Systems for Video Technology*, .

Xu, K., Li, C., Tian, Y., Sonobe, T., Kawarabayashi, K.-i., & Jegelka, S. (2018). Representation learning on graphs with jumping knowledge networks. In *International conference on machine learning* (pp. 5453–5462). PMLR.

Xu, L., Ouyang, W., Bennamoun, M., Boussaid, F., Sohel, F., & Xu, D. (2021). Leveraging auxiliary tasks with affinity learning for weakly supervised semantic segmentation. In *Proceedings of the IEEE/CVF International Conference on Computer Vision* (pp. 6984–6993).

Xu, L., Ouyang, W., Bennamoun, M., Boussaid, F., & Xu, D. (2022b). Multi-class token transformer for weakly supervised semantic segmentation. In *Proceedings of the IEEE/CVF Conference on Computer Vision and Pattern Recognition* (pp. 4310–4319).

Yao, Y., Chen, T., Xie, G.-S., Zhang, C., Shen, F., Wu, Q., Tang, Z., & Zhang, J. (2021). Non-salient region object mining for weakly supervised semantic segmentation. In *Proceedings of the IEEE/CVF Conference on Computer Vision and Pattern Recognition* (pp. 2623–2632).

Ying, Z., You, J., Morris, C., Ren, X., Hamilton, W., & Leskovec, J. (2018). Hierarchical graph representation learning with differentiable pooling. *Advances in neural information processing systems*, *31*.

You, R., Guo, Z., Cui, L., Long, X., Bao, Y., & Wen, S. (2020). Cross-modality attention with semantic graph embedding for multi-label classification. In *Proceedings of the AAAI conference on artificial intelligence* (pp. 12709–12716). volume 34.

Zhang, B., Xiao, J., Jiao, J., Wei, Y., & Zhao, Y. (2021a). Affinity attention graph neural network for weakly supervised semantic segmentation. *IEEE Transactions on Pattern Analysis and Machine Intelligence*, *44*, 8082–8096.

Zhang, D., Zhang, H., Tang, J., Hua, X.-S., & Sun, Q. (2020a). Causal intervention for weakly-supervised semantic segmentation. *Advances in Neural Information Processing Systems*, *33*, 655–666.

Zhang, F., Gu, C., Zhang, C., & Dai, Y. (2021b). Complementary patch for weakly supervised semantic segmentation. In *Proceedings of the IEEE/CVF International Conference on Computer Vision* (pp. 7242–7251).

Zhang, J., Li, W., & Li, Z. (2022). Distinguishing foreground and background alignment for unsupervised domain adaptative semantic segmentation. *Image and Vision Computing*, *124*, 104513.

Zhang, J., Li, Z., Zhang, C., & Ma, H. (2020b). Robust adversarial learning for semi-supervised semantic segmentation. In *2020 IEEE International Conference on Image Processing (ICIP)* (pp. 728–732). IEEE.

Zhang, J., Li, Z., Zhang, C., & Ma, H. (2021c). Stable self-attention adversarial learning for semi-supervised semantic image segmentation. *Journal of Visual Communication and Image Representation*, *78*, 103170.

Zhang, L., Li, X., Arnab, A., Yang, K., Tong, Y., & Torr, P. H. (2019). Dual graph convolutional network for semantic segmentation. *arXiv preprint arXiv:1909.06121*, .

Zhao, H., Shi, J., Qi, X., Wang, X., & Jia, J. (2017). Pyramid scene parsing network. In *Proceedings of the IEEE conference on computer vision and pattern recognition* (pp. 2881–2890).

Zhou, Q., Feng, Z., Gu, Q., Pang, J., Cheng, G., Lu, X., Shi, J., & Ma, L. (2022). Context-aware mixup for domain adaptive semantic segmentation. *IEEE Transactions on Circuits and Systems for Video Technology*, .

Zhou, T., Li, L., Li, X., Feng, C.-M., Li, J., & Shao, L. (2021). Group-wise learning for weakly supervised semantic segmentation. *IEEE Transactions on Image Processing*, *31*, 799–811.